Paper presented at the 22nd Asian Conference on Remote Sensing, 5 - 9 November 2001, Singapore.

THE USE OF HYPERSPECTRAL DATA IN IDENTIFYING "DESERT-LIKE" SOIL SURFACE FEATURES IN TABERNAS AREA, SOUTHEAST SPAIN

Dante E. Margate[1] and Dhruba P. Shrestha[2]
[1] Bureau of Soils and Water Management, Quezon City, Philippines
[2] International Institute for Aerospace Survey and Earth Sciences,
P O Box 6, 7500 AA Enschede, The Netherlands
Emails: danmargz@hotmail.com; Shrestha@itc.nl

KEY WORDS: Hyperspectral data, Spectral Angle Mapper, desert-like surface features

ABSTRACT: The potential use of hyperspectral data in mapping "desert-like" surface features was undertaken in a semi-arid area of Tabernas area in Southeastern part of Spain. "Desert-like" soil surface features like desert pavements, surface accumulation of salts, calcium carbonate accumulation, and surface exposure of gypsum materials are manifestations of some kind of land deterioration in semi-arid regions. Mapping the spatial distribution and extent of these features would be relevant in different aspects of environmental studies especially in areas vulnerable to land degradation in arid regions. Field spectral measurements carried out on the identified surface features, together with spectral measurements at laboratory conditions, were analysed to establish specific spectral response of each target. Established reflectance curves, after matching with image spectra, were then used to classify an atmospherically corrected airborne hyperspectral data of the area. Spectral Angle Mapper, an algorithm that compares image spectra and individual spectra of specified targets, was applied. The spatial distribution of each "desert-like" soil surface feature was verified to the soil-landscape pattern of the area.

1. INTRODUCTION

Land degradation is a major problem in many Mediterranean regions. The environment, with droughts of up to 11 months, torrential rains, pronounced relief, soft bedrock, and shallow soils throughout the area makes it inherently vulnerable to a wide range of land degradation processes (Boer, 1999). The area of Southeast Spain is of no exception, with its semi-arid climate, long hot summers, and annual precipitation of less than 350 mm. The high annual potential evapotranspiration rates, that always exceed annual precipitation, result in a less vegetative cover for surface protection. Soil erosion, salinization, flooding and sedimentation, depletion of soil nutrients and pollution are among the few processes contributing to deterioration of the land. The concept of desertification, considered a severe stage of land degradation, is responsible for the manifestation of "desert-like" conditions especially in dryland areas outside the desert boundaries (Rapp, 1986). Desert pavements, which are continuous layer of gravel and small stones, are usually formed on the surfaces of the pediments, fans and plains. Due to the high evaporation rates, lack of leaching and percolation to deeper horizons, many areas of the semi-arid regions are saline and alkaline (Boer, 1999). Calcium carbonate and gypsum are often present in abundance, forming nodules or hardpans and contributing to the formation of surface crusts (Courty, 1993).

Hyperspectral remote sensing renders a different approach in image processing techniques. Conventional broadband sensors such as SPOT, Landsat MSS and Landsat TM are not very suitable for mapping soil properties because their bandwidth of 100 to 200 μm cannot resolve diagnostic spectral features of terrestrial materials (De Jong, 1994). Analytical techniques developed for analysis of broadband spectral data may be incapable of taking advantage of the full range of information present in hyperspectral remote sensing imagery (Cloutis, 1996). Increased spatial resolution also facilitates detailed surficial mapping. This study aims to identify and determine the spatial distribution of the so-called "desert-like" soil surface features present in the study area according to their spectral responses. Field and laboratory spectral measurements were used to classify the hyperspectral data in order to map the mentioned features.

2. STUDY AREA

The study area is located in the small town of Tabernas in the province of Almeria (Figure 1). The exact site corresponds to the coverage of the HYMAP airborne hyperspectral image, with its flight line starting at 37°02'32" N and 2°30'14" W and ending at 37°04'25" N and 2°16'40" W. It covers a rectangular area of around 8,000 hectares with dimensions of 4 km width and 20 km length. The climate is characterised as semi-arid with long hot summers. Annual precipitation varies from 115 mm to 431 mm, with rainy days varying from 25 to 55 days. The terrain is relatively rugged and devoid of vegetation.

Figure 1: The study area

The soils in general are shallow (less than 50 cm depth), except in the valleys and occasionally on the piedmonts. Soil texture is commonly sandy loam to loamy sand with more than 40% coarse fragments on the surface. Saline soils occur in the valleys with electrical conductivity values of more than 2 dS/m. Surface crusting is common particularly in saline areas. Most of the soils are strongly calcareous with calcium carbonate content ranging from 2-31%. Soils in the hillands and piedmonts are classified as Lithic Torriorthents, and the deeper soils are classified as Typic Torriorthents according to the USDA Soil Taxonomy (Soil Survey Staff, 1998). In the valleys, soils are classified as Fluventic Haplocambids and towards the upper terraces, as Typic Haplocambids.

3. MATERIALS AND METHODS

A HYMAP hyperspectral image of the study area, acquired on 2 June 1999, was made available by DLR (German Aerospace Center). The data was acquired at an altitude of 3350 m above ground. The HYMAP scanner has four individual spectrometers along the wavelength range of 400 to 2500 nm. The spectrometers cover this wavelength range by 128 spectral bands with a bandwidth of approximately 16 nm. The spatial resolution varies from 5 to 10 m.

Spectral measurements in the field and in laboratory condition were accomplished by using the GER-3700 Spectroradiometer, which has a full real-time data acquisition of 647 channels along the 350 to 2500 nm wavelength. Reflectance spectra were obtained by comparing the radiance of the target with the radiance of a reference panel ($BaSO_4$ panel). Target and reference scans were made successively and compared automatically to produce reflectance measurements. Field observation and soil description were performed in the selected sites. Surface soil samples were collected for spectral measurements at laboratory conditions and for laboratory analyses of some chemical and physical soil properties such as particle size distribution, pH, electrical conductivity (EC), percent gypsum, percent calcium carbonates, percent total organic carbon, and percent organic matter content.

Spectral measurements at laboratory conditions were carried out using a 500 watts halogen lamp as light source positioned at about 15^o zenital angle. Samples were placed on a black background. Spectra obtained from the laboratory were used to derive reflectance characteristics.

Visualisation and extraction of the absorption feature parameters (wavelength position, depth, width, area, and asymmetry) for every spectrum were performed in PIMAVIEW software. “Statistics” function was applied for the automatic detection and calculation of these absorption feature parameters. Statistical correlation coefficients were computed between the measurable soil variable and the absorption feature parameters at obtained wavelength intervals characteristic of a certain soil parameter. Pearson product moment correlation coefficient was used to measure the degree of linear relationship. A two-tailed test of the correlation was computed and presented as p-values. A p-value of less than 0.05 indicates that the correlation is significant at more than 95% level.

Spectral Angle Mapper (SAM) was used to classify the hyperspectral data. In SAM, classification is carried out by comparing image spectra to individual spectra or a spectral library (Kruse et al., 1993). It assumes that the data have been reduced to apparent reflectance (true reflectance multiplied by some unknown gain factor controlled by topography and shadows). The algorithm determines the similarity between two spectra by calculating the "spectral

angle" between them, treating them as vectors in a space with dimensionality equal to the *n* number of bands (Figure 2),

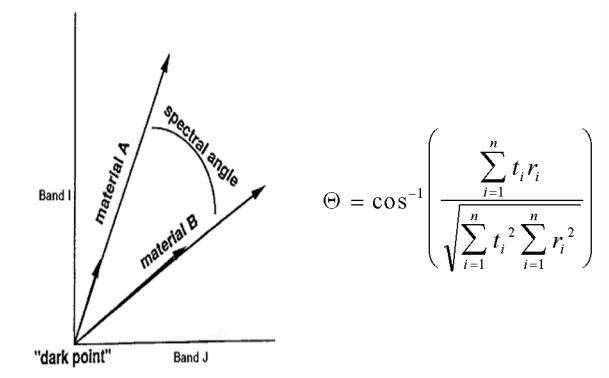

$$\Theta = \cos^{-1}\left(\frac{\sum_{i=1}^{n} t_i r_i}{\sqrt{\sum_{i=1}^{n} t_i^{\,2} \sum_{i=1}^{n} r_i^{\,2}}}\right)$$

Figure 2: Two -dimensional illustration on the concept of SAM function and the calculation of spectral angle

Since it uses only the "direction" of the spectra, and not their "length," the method is insensitive to the unknown gain factor, and all possible illuminations are treated equally. Poorly illuminated pixels will fall closer to the origin. The "colour" of a material is defined by the direction of its unit vector. Notice that the angle between the vectors is the same regardless of the length. The length of the vector relates only to how fully the pixel is illuminated. The SAM algorithm generalises this geometric interpretation to *n* - dimensional space. SAM determines the similarity of an unknown spectrum *t* to a reference spectrum *r*, where the spectral angle Θ, between the two spectra as calculated for each channel, *i*, is determined for every image spectrum (pixel) (CSES, 1992). This value, in radians, is assigned to the corresponding pixel in the output SAM image, one output image for each reference spectrum. Rule images (end member maps) were produced using a 0.1 radians threshold angle for matching the reference spectrum to the unknown image spectra and the hyperspectral classification was achieved by using all spectra of the surface features simultaneously for the SAM algorithm.

4. RESULTS AND DISCUSSIONS

4.1 "Desert-like" Soil Surface Features

Large areas having desert pavements were recognised towards the western part of the study area. Surface accumulation of wind-polished, closely packed rock fragments overlying a more or less homogeneous fine sandy loam soils were observed generally on the upper terraces of the valleys. The residual concentration of coarse fragments is a result of continuous removal of finer materials from the surface by wind action and presumably due to sheet wash during flash floods.

Saline soils were easily identified in the field due to its distinct appearance. The formation of salt crust in the surface, a "puffy" feeling when stepping on it, and the presence of halophytic plants like *Salicornia sp*. and *Salsola sp*. were among the major indicators. A field EC meter also provided an estimate of the electrical conductivity of the sample. However, laboratory analysis of EC was used to confirm the identification of this soil feature.

The presence of calcium carbonates ($CaCO_3$) on the soil surface was determined using a 10% HCl solution. Most of the areas have strong reaction with the acid, except for some soils derived from non-calcareous parent materials. The non-calcareous soils are located towards the eastern side, frequently on the valleys. These soils developed from the parent material consisting of mica schists, gneiss, and quartzites, which were washed down by flash floods. Although calcareous soils are extensive, distinct appearance on the soil surface could not be seen.

Surface accumulation of secondary gypsum was not detected. Exposed primary gypsum located at both ends (western and eastern) of the study area, was however recognised. A very thin soil (few cm depth) evolved at the surface from the weathering of the gypsum parent material.

Formation of surface crusts is common on Mediterranean soils. High evaporation rates and the presence of salts in important amounts contribute to the development of crusting. Indeed, extensive areas in the entire study site exhibited surface crusting in varying degree. However, it was observed that most of the soils forming crusts on the surface are soils with EC values of more than 2 dS/m. Consequently, assumptions were deduced on the direct relationship of surface crusting and saline soils on this area.

4.2 Spectral Response of Soils

Image spectra were established for each "desert-like" soil surface features after confirming the appropriate match between field/laboratory spectra and pixel spectra. The established spectra for each surface feature are shown in Figure 3.

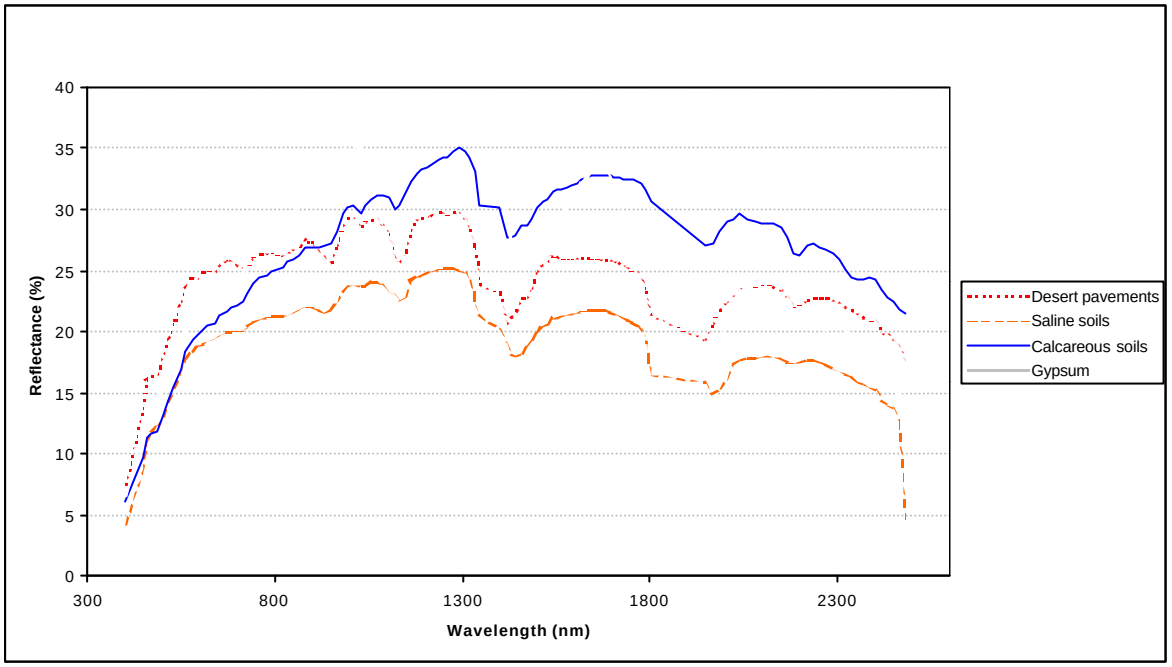

Figure 3: Established image spectra of the identified "desert-like" soil surface features

Diagnostic absorption features of soils are due to the inherent spectral behaviour of the mineralogical composition, organic matter, and water according to several literatures (Baumgardner et al., 1985 and Irons et al., 1989). Prominent absorption bands around 1450 nm and 1950 nm wavelength in most soil spectra are attributed to water and hydroxyl ions. Occasional weaker absorption bands caused by water also occur at 970, 1200, and 1770 nm. Absorption features near the 400 nm wavelength for all samples are also noticeable. Absorption bands at 1800 and 2300 nm are attributed to gypsum, while strong absorption feature near 2350 nm are assigned to calcite ($CaCO_3$). Several absorption features are also attributed to the presence of iron in both ferric and ferrous form. Noticeable features occur at around 700, 900, and 1000-1100 nm of the wavelength.

Saline soils exhibited significantly higher reflectance values all throughout the 325 to 2500 nm wavelength of the spectrum. This conforms to the study of Stoner (1979), which indicated that soils specifically Aridisols, with high amount of soluble salts, gave the highest average reflectance than soils with low salt content. But strongly saline soil sample displayed very low reflectance intensity throughout the entire spectrum as compared to moderately saline soils. The main reason for this phenomenon is due to the higher amount of moisture present in the sample during spectral measurements. Furthermore, stronger water absorption features around 1400 and 1900 nm of the spectrum for strongly saline soils convincingly support this claim. Absorption bands at 390-400, 615-625, 685-695, 800-810, 950-960, 1410-1420, 1935-1945, and 2350-2360 nm wavelengths were selected and correlated with EC values. Pearson product moment correlation coefficients with the corresponding p-values are presented in table 1. Significant correlation coefficients were observed for EC values with depth, width, and asymmetry at wavelength of 800-810 nm. This implies that the depth of the absorption feature at this specific wavelength interval increases with the degree of salinity, while the width and asymmetry at this feature decrease with increasing EC values. Hence, absorption features found on the 800-810 nm wavelength interval would significantly be affected by the amount of salts present in the soils.

The diagnostic absorption features of the gypsum spectra from the libraries are also very distinct in the reflectance spectrum of the sample. The difference in the illumination and the degree of weathering may have caused the relatively lower reflectance values of the sample. Strong absorption features that characterise gypsum in the wavelength intervals near 1750, 1940, 2200 and 2400 nm, are results of vibrational processes of water. Characteristic features at 990, 1200, 1440, 1480 and 1530 nm are also overtones and combination of OH stretching

in water. The characteristic doublet peak around 1440 to 1540 nm of a gypsum mineral is also clearly observable in the sample spectrum.

Table 1: Correlation matrix between EC and absorption feature parameters at selected absorption bands.

Wavelength (10 nm intervals)	Number of samples	Wave	Depth	Width	Area	Asymmetry
390-400	31	-0.431	0.346	-0.325	0.269	-0.176
		0.015	0.057	0.075	0.144	0.342
615-625	5	0.437	0.997	0.432	0.603	0.344
		0.462	0.000	0.467	0.282	0.570
685-695	9	-0.222	0.279	-0.168	0.173	-0.322
		0.566	0.467	0.666	0.656	0.397
800-810	13	0.343	0.891	-0.901	-0.526	-0.845
		0.251	0.000	0.000	0.065	0.000
950-960	10	0.531	0.593	-0.009	0.637	-0.443
		0.114	0.071	0.981	0.048	0.200
1410-1420	31	0.127	0.054	-0.176	-0.115	-0.159
		0.495	0.773	0.343	0.537	0.393
1935-1945	22	0.233	0.420	-0.066	0.101	-0.186
		0.296	0.052	0.771	0.655	0.408
2350-2360	18	0.365	-0.089	-0.067	0.112	-0.288
		0.137	0.726	0.790	0.658	0.246

Table 2: Correlation matrix between percent gypsum and selected diagnostic absorption features of gypsum

Wavelength (10 nm interval)	n	Wave	Depth	Width	Area	Asymmetry
982-1002	14	0.519	0.650	-0.391	0.083	0.830
		0.057	0.012	0.167	0.777	0.000
1174-1210	7	0.509	0.826	-0.590	-0.481	0.370
		0.243	0.022	0.163	0.274	0.414
1434-1454	8	0.169	0.975	-0.231	0.248	-0.313
		0.689	0.000	0.583	0.554	0.450
1734-1754	15	0.419	0.831	-0.516	-0.058	0.220
		0.120	0.000	0.049	0.837	0.430
1926-1946	25	0.053	0.280	-0.121	0.045	-0.212
		0.802	0.175	0.563	0.830	0.310
2162-2214	37	0.105	0.723	0.660	0.897	-0.064
		0.538	0.000	0.000	0.000	0.707

The correlation matrix in Table 2 explains the relationship of the diagnostic absorption features to the gypsum content of the samples at characteristic wavelength intervals for gypsum mineral. Depth of the absorption feature varies significantly with gypsum content in almost all selected wavelength intervals. At wavelength position near 2200 nm, depth, width, and area changes significantly with gypsum content.

A strong absorption feature of calcium carbonates is manifested near 2350 nm wavelength, which is due to the vibrational processes of the carbonate ion (CO_3^{2-}) and water. Overtone bands also produced by vibrational processes are located at 2120-2160 nm, 1970-2000 nm, and 1850-1870 nm. No significant correlations were however observed, except that of wavelength interval 1720-1780 nm and absorption width, and interval 2140-2210 nm and asymmetry.

4.3 Hyperspectral Image Classification

The spatial distributions of each soil surface features are mapped individually. Final classification result is shown in figure 4. Extensive areas were classified to be calcareous soils comprising around 40% of the total area. Saline soils occupy 17% whereas desert pavements cover 11% of the entire study area. Unclassified pixels of about 12% coincided with the location of the vegetation cover.

The mapping of calcareous soils was quite difficult since there was no distinguishing surface feature to identify the accumulation of calcium carbonates. The identified area was based on a spectrum with barely 20% carbonate

content, which shows absorption feature at 2350 nm wavelength. The identification of the exposed gypsum at both ends of the study area was expected to come out easily.

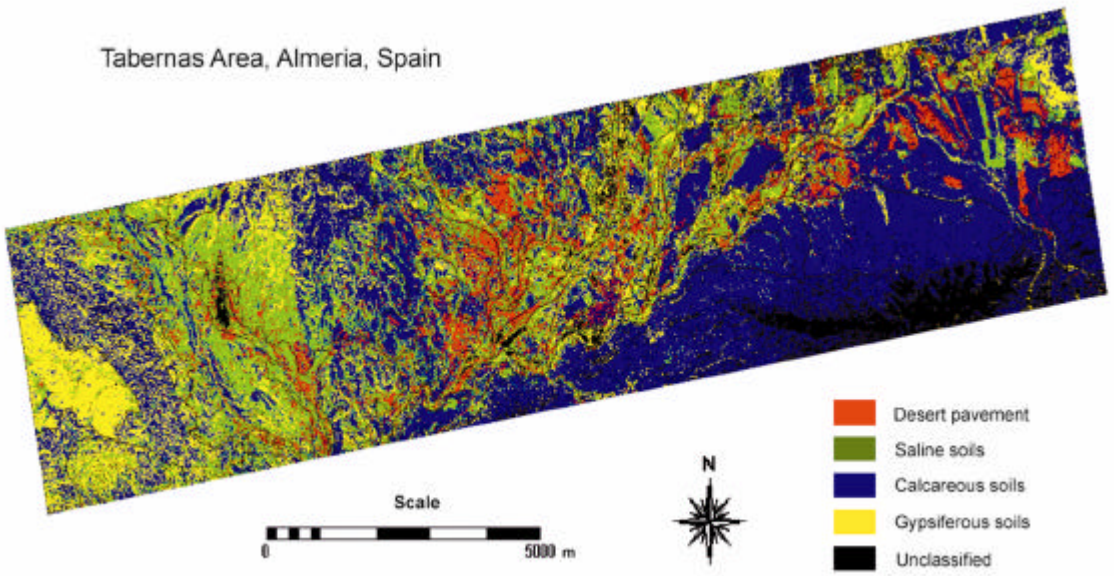

Figure 4: Classification result

5. CONCLUSION

The use of hyperspectral data proved to be promising in determining the spatial distributions of the identified "desert-like" soil surface features. The presence of desert pavements, saline soils, calcareous soils, and exposed gypsum somehow indicate that the area is slowly undergoing a process of desertification. However, this kind of land deterioration given the physical setting, geologic composition and climatic condition of the area, was identified more of a natural process rather than consequences of man's activities. Reflectance properties of soils were significantly influenced by the different surface features present in the area, although not necessarily characterising desertification as such. Spectral angle mapper algorithm for classifying hyperspectral images proved to be reasonable in mapping "desert-like" soil surface features.

6. REFERENCES

Baumgardner, M.F., L.F. Silva, L.L. Biel, and E.R. Stoner. 1985. Reflectance properties of soils. Adv. in Agronomy. 38: 1-44.

Boer, M.M. 1999. Assessment of dryland degradation: Linking theory and practice through site water balance modelling. Netherlands Geographical Studies. KNAG, Utrecht. 304 pp.

Center for the Study of Earth from Space (CSES). 1992. SIPS User's Guide, The spectral image processing system. Vol. 1.1. University of Colorado, Boulder. 74 p.

Cloutis, E.A. 1996. Hyperspectral geological remote sensing: evaluation of analytical techniques. Int. J. Remote Sensing. 17(12): 2215-2242.

Courty, M.A. 1993. Morphology and genesis of soil surface crusts in semi-arid conditions. In: Proceedings of the International Symposium on the assessment of soil surface sealing and crusting. Ghent, Belgium 1985. pp. 32-39.

De Jong, S.M. 1994. Applications of reflective remote sensing for land degradation studies in a mediterranean environment. Netherlands Geographical Studies. KNAG, Utrecht. 240 pp.

Irons, J.R., R.A. Weismiller, and G.W. Peterson. 1989. Soil reflectance. In: G. Asrar. Theory and applications of optical remote sensing. Wiley, New York. pp. 66-110.

Kruse, F.A., A.B. Lefkoff, J.W. Boardman, K.B. Heidebrecth, A.T. Shapiro, J.P. Barloon, and A.F. Goetz. 1993. The spectral image processing system (SIPS) – Interactive visualization and analysis of imaging spectrometer data. Remote sensing of environment. 44: 145-163.

Rapp, A. 1986. Introduction to soil degradation processes in drylands. Climatic Change 9. pp 19-31.

Soil Survey Staff. 1998. Keys to soil taxonomy. 8th edition. USDA Natural Resources Conservation Service, Washington. 326 pp.

Stoner, E.R. 1979. Physico-chemical, site, and bidirectional reflectance factor characteristics of uniformly moist soils. Ph.D. dissertation. Purdue Univ.,West Lafayette, Indiana